🔓 **Open Access**

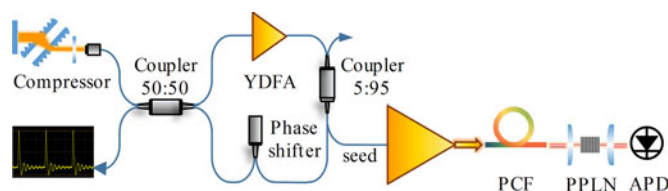# Octave-Spanning Supercontinuum Generation From an NALM Mode-Locked Yb-Fiber Laser System

Zhengru Guo
Qiang Hao
Song Yang
Tingting Liu
Hong Hu
Heping Zeng

Octave-Spanning Supercontinuum Generation From an NALM Mode-Locked Yb-Fiber Laser System

Zhengru Guo,[1] **Qiang Hao,**[1] **Song Yang,**[1] **Tingting Liu,**[1] **Hong Hu,**[2] **and Heping Zeng**[3]

[1]Shanghai Key Laboratory of Modern Optical Systems and Engineering Research Center of Optical Instrument and Systems, Ministry of Education, School of Optical Electrical and Computer Engineering, University of Shanghai for Science and Technology, Shanghai 200093, China

[2]Department of Pulmonary Medicine, Chinese PLA General Hospital, Beijing 100853, China

[3]State Key Laboratory of Precision Spectroscopy, East China Normal University, Shanghai 200062, China, and Shanghai Key Laboratory of Modern Optical Systems and Engineering, Research Center of Optical Instruments and Systems, Ministry of Education, School of Optical-Electrical and Computer Engineering, University of Shanghai for Science and Technology, Shanghai 200093, China

Abstract: We demonstrate a broadband all polarization-maintaining Yb-fiber laser system that provides 137-nJ pulse at 140-fs duration. The pulses are generated in a passively mode-locked laser in which the nonlinear amplifying loop mirror acts as the mode locker, an integrated nonreciprocal device biases $\pi/2$ phase shift to reduce the mode locking threshold, and a pair of gratings are involved to force the oscillator operating in its quietest mode. Self-started mode locking is first achieved in multiple-pulse regime with 250-mW pump power, and stable single-pulse operation with 1.1-ps pulse duration, 75-pJ energy, and 29-nm spectral width are obtained subsequently when the pump power is decreased to 135 mW. Being amplified and spectral broadened, the laser pulses lead to an f_{ceo} signal with $>$30-dB signal-to-noise ratio (SNR) which is suitable for frequency comb stabilization.

Index Terms: Fiber Lasers, mode-locked laser, ultrafast laser, supercontinuum generation.

1. Introduction

Since the extremely accurate longitudinal frequency and ultra-narrow comb-linewidth, optical frequency comb is finding an increasing number of applications in a plethora different areas such as the frequency metrology, distance measurement, optical molecular spectroscopy, optical clock and astronomical observation [1]–[6]. Recently, passively mode-locked fiber lasers greatly highlight the generation of frequency comb due to their compact size, easy manufacturability, stable operation and high performance [7], [8]. Real saturable absorbers (SA), such as the semiconductor saturable absorber mirror (SESAM), graphene, and carbon nanotubes are commonly used for mode locking

[9]–[13]. However, limited by the relatively low damage threshold, complicated fabrication and a gradual degradation over time, the SA materials are confined within the laboratory application [11].

Artificial SA is an alternative way for passively mode locking. The most popular configuration is the nonlinear polarization evolution (NPE) mechanism which is quite convenient to build with conventional fiber and bulk components. To date, NPE mode-locked fiber oscillators working in stretched-pulse regime have produced the pulse duration down to seven optical cycles at both 1.0 and 1.55 μm [14], [15]. However, one of the primary drawbacks of NPE lasers is caused by the employment of discrete spatial optics and non-polarization maintaining (non-PM) single-mode fiber which bring the sensitivity of external perturbations, such as temperature variation and mechanical stress. Benefitted from the outstanding stability and immunity in rugged environment, all PM fiber lasers have been rapidly improved [9], [16]. It has been found that long enough PM-fiber has to be used to accumulate large enough phase for mode locking so as to the repetition rate is limited to 10 MHz, unless a SESAM is used [17], [18].

Furthermore, fiber laser mode-locked by means of nonlinear amplifying loop mirror (NALM) with a figure-of-eight architecture has been investigated to be a promising candidate for all PM configuration with intrinsic low noise [19]–[21]. In these systems, the phase shift $\triangle\varphi$ between the clockwise and anticlockwise propagating pulses in the nonlinear loop plays the most significant role for self-started mode locking, thus relatively long PM fiber and high enough pump power are necessary [22]–[24]. Besides, an active modulator, such as acousto-optic modulator, or mechanical tapping would sometimes help to force pulse formation [25], [26]. Recently, as low as 100-μHz standard deviation of stabilized repetition rate is achieved in a dispersion-imbalanced NALM via pump-induced refractive index change [27].

To shorten the cavity length and reduce the mode locking threshold of figure-of-eight laser cavities, Lin *et al.* proposed a manually adjustable nonreciprocal phase shifter to release the requirement on nonlinear phase shift [28]. In a phased-biased NALM, the phase shifter offered a linear phase difference of $\triangle\varphi_L$ between the clockwise and anticlockwise propagating pulses, while the Kerr effect caused a nonlinear phase difference of $\triangle\varphi_N$. The overall phase difference $\triangle\varphi$ is the sum of $\triangle\varphi_L$ and $\triangle\varphi_N$. When the overall phase difference accumulated to $n\pi$, where n is an odd number, the laser fully transmits and the cavity loss achieves the minimum. Conversely, in the figure-of-nine laser cavity, the n need to be an even number. Recently, a transmission type non-reciprocal phase shift device with discrete optics was developed [29]. Additionally, a phase-biased NALM mode-locked Er-fiber comb operating in the stretched-pulse regime shows an integrated timing jitter of 40 as from 10 kHz to 10 MHz [30]. As for 1.0 μm wavelength, a narrow band spectrum filter has to be used to reset the pulse characters at the end of each roundtrip so as to "compensate" for the large dispersion in all normal dispersion regime [22], [29]. Although a phase-biased device can greatly decrease the mode locking threshold, the 2.8-nm filter (or a 300 l/mm grating acted as filter) is still necessary to play the significant role in pulse formation, and hence the spectral width and the compressed pulse is limited to 3.1 nm (8 nm) and 538 fs (1.1 ps) [31]. What's more, the interference effect always produce rugged spectrum at the free port of the 2 × 2 bridge coupler for NOLM or NALM [31], [32]. For frequency comb generation, the pulse shaping in the stretched-pulse regime is desired, for the oscillators with the zero net cavity-dispersion have shown the lowest level of timing jitter, narrowest linewidth and quiet noise of f_{ceo} [33]. Therefore, a self-started Yb-fiber laser with both low threshold and broadband spectrum within all PM fiber architecture is urgently needed.

In this paper, we demonstrate an all PM NALM mode-locked laser system for the aim of a robust frequency comb generation. A π/2 phase shifter was inserted in the nonlinear loop to reduce the mode locking threshold and a compactible grating-pair was employed in the linear arm to manage the cavity dispersion. With an optimized separation of the grating pair, the spectral width is achieved as broad as 29 nm. The 2.3-mW output power from laser oscillator was effectively scaled by a Yb-doped PM photonics crystal fiber to more than 8 W. The amplified pulse can be dechirped to 140 fs duration with >60% compression efficiency. A 9-cm long high nonlinearity PCF and a semi-collinear *f-2f* interferometer are employed to produce an octave-spanning SC and the f_{ceo} beating signal.
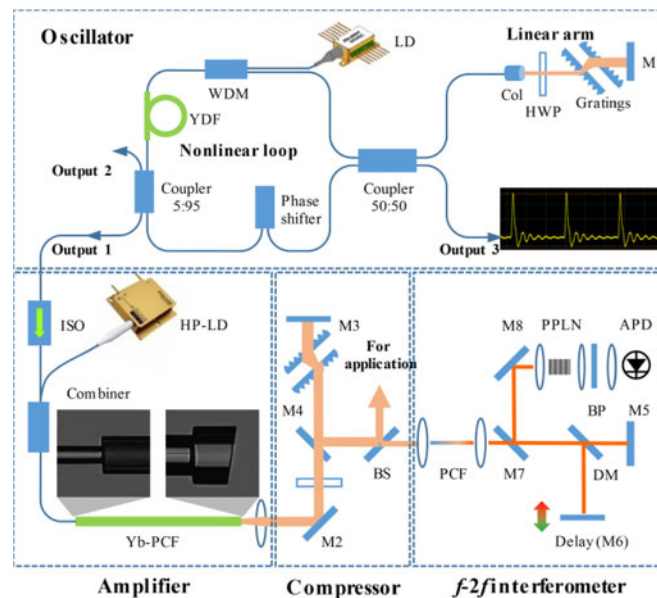
Fig. 1. Schematic configuration of the Yb-fiber laser system. LD: 400-mW laser diode; WDM: wavelength division multiplexer; YDF: Yb-doped fiber; Col: collimator; HWP: half wave plate; ISO: isolator; HP-LD: 27-W laser diode; Yb-PCF: Yb-doped photonic crystal fiber; M1-M4: mirrors with high reflection from 1020-1080 nm; BS: beamsplitter; M5-M8: golden mirrors; PPLN: periodically poled lithium niobate; DM: dichroic mirror; BP: bandpass filter; APD: avalanche photo-detector.

2. Experimental Setup and Results

Fig. 1 outlines the schematic of the laser system, including a NALM mode-locked oscillator, a Yb-doped photonics crystal fiber (PCF) amplifier in all-fiber architecture, a grating-pair pulse compressor, and an *f*-2*f* interferometer. All fibers and pigtails of fiber components are polarization maintaining. The NALM mode-locked laser oscillator consists of a nonlinear loop and a linear arm. A 1.5-m long Yb-doped fiber (PM-YSF-HI, Nufern) asymmetrically located in the nonlinear loop acts as the gain media and provides the differential nonlinear phase shift. The Yb-doped fiber is pumped by a 976-nm laser diode with a maximum pump power of 400-mW via a 980/1030 nm wavelength division multiplexer (WDM). Two 5% branches of a 2 × 2 coupler with 5:95 splitting ratio act as the output port. The output-1 acts as the seed laser for the amplifier while the output-2 acts as monitor port. A reflection-type phase shifter working at 1064 nm is employed to provide a non-reciprocal phase shift of $\pi/2$. The linear arm is composed of a collimator (Col), a half wave plate (HWP), a pair of transmission gratings, and a high reflection mirror (M1). The grating used in cavity has a grating patch of 800 nm (1250 l/mm) and a diffraction efficiency of ∼90% per pass. The nonlinear loop and linear arm are connected by another 2 × 2 coupler with 50:50 splitting ratio. The output-3 of the 50:50 coupler acts as another monitor port.

The self-started mode locking firstly operated in multiple-pulse regime when the pump power was ramped up to 250 mW. Single pulse operation could be achieved by carefully decreasing the pump power to 135 mW. The mode locking would vanish when the pump power is lower than 110 mW. With 4.5-m long fiber in nonlinear loop, 0.5-m long fiber in linear arm, and 0.07-m spatial separation, the oscillator worked at a fundamental repetition rate of 36.7 MHz. In order to obtain a suitable spectrum for power amplification, we investigated the output characters of three output ports, output-1, output-2, and output-3. Fig. 2(a) illustrates the measured spectral profiles at the pump power of 135 mW. Note that all the three spectra show identical spectral edge but different spectral top. Owing to the phase-biased NALM in figure-of-nine cavity transmits most of the CW components and partial of the laser pulse, the optical spectrum of output-3 (black curve in Fig. 2(a)) shows only 20 dB spectral signal-to-noise ratio (SNR). While the spectrum measured at output-1 shows approximate 30 dB spectral SNR. The output powers measured from output 1, 2 and 3 were
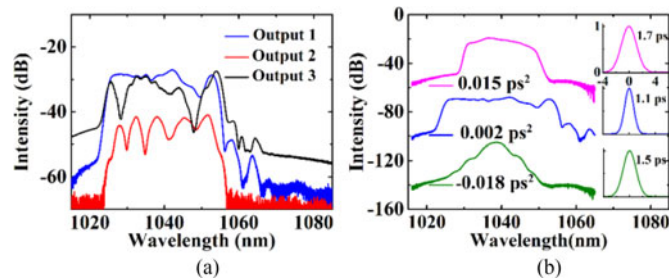
Fig. 2. (a) Spectral profiles measured at different output ports. (b) Spectral profiles of output 1 with different cavity net-dispersion. (Inset) The corresponding autocorrelation traces.

2.3, 0.08 and 1.2 mW, respectively. Empirically, the pulse from output-1 is in favor of the following amplification.

Considering that the f_{ceo} signal strongly related to the cavity net-dispersion, we optimized separation of the intra-cavity gratings. The YDF and PM 980 fiber used in the oscillator have a group velocity dispersion (GVD) of $\sim$26 fs^2/mm and a third-order dispersion (TOD) of $\sim$41 fs^3/mm. Totally, the group delay dispersion contributed by 5-m long fibers was calculated to be 0.13 ps^2. While the GVD and TOD of grating pairs were calculated to be -1.35×10^4 fs^2/mm and 5.3×10^4 fs^3/mm, respectively. The broadest spectrum was 29 nm at full width at half maximum (FWHM) when the grating separation is 9.5 mm, corresponding to a net cavity-dispersion of 0.002 ps^2. The pulse width was measured to be 1.1 ps [see the blue curves in Fig. 2(b)]. Increasing or decreasing the grating separation will both lead to spectrum narrowing and pulse lengthening. With a net dispersion of -0.018 ps^2, the laser oscillator operated in the soliton regime, and the output spectrum shows a lightly sidebands due to the periodical soliton perturbation [see the green curves in Fig. 2(b)]. While in normal dispersion regime with 0.015 ps^2 net dispersion, the pulse duration stretches to 1.7 ps, and the spectrum shows steep edges [see the pink curves in Fig. 2(b)].

For supercontinuum generation and f_{ceo} detection, $\sim$nJ pulse energy within $\sim$100 fs pulse duration is preferred. Therefore, an all-fiber amplifier as well as pulse compressor was installed after the oscillator, as illustrated in Fig. 1. The amplifier is composed of a high power isolator (ISO), a pump-signal combiner, and a single-mode PM double-clad Yb-doped photonics crystal fiber (PCF). The fiber for the common port of the combiner is double cladding fiber with a core/cladding diameter of 6/125 μm. To ensure a robust and compact power amplifier, the components in the fiber amplifier were coupled with PM fibers and successively spliced, ensuring low insertion loss and high polarization extinction ratio. The Yb-doped PCF which has a mode field diameter (MFD) of 15 μm, a pump cladding diameter of 135 μm, and a cladding absorption of $\sim$7 dB/m at 976 nm was directly spliced to the common port of the combiner. With a slightly collapse at the input port of the PCF (see the inset picture in Fig. 1), the splice losses for the pump and signal beams were both minimized to less than 1 dB. To improve damage threshold of the end face, an endcap (coreless fiber) with 260-μm length and 400-μm diameter was spliced to the end of PCF fiber. Moreover, the endcap was cleaved with 8° angle (zoomed in Fig. 1) to suppress self-oscillation. In order to provide enough gain while minimize nonlinear distortion, the length of the Yb-doped PCF was optimized to 1-m length. Under 20-W pumping power, the signal laser was amplified to 8 W average power with a slope efficiency of 40% (see Fig. 3(a)). The optical spectrum remained unchanged when the output power is scaled from 3 to 8 W (see Fig. 3(b)), indicating that the amplifier operated in low noise regime.

To dechirp the amplified pulse, a lens with 8-mm focus length was employed to collimate the fiber laser into free-space. Another pair of gratings (same as the dispersion line in the oscillator) is precisely adjusted to compress the chirped pulses. With a grating separation of 10 mm, the 9.4 ps pulse from the amplifier (see the red curve in the inset of Fig. 3(c)) was dechirped to 140 fs in duration (see the blue curve in Fig. 3(c)). Considering a 23.5-nm spectral width (see the red curve in Fig 3. (b)), the time-bandwidth product is calculated to be 0.992 which is more than 2 times of the
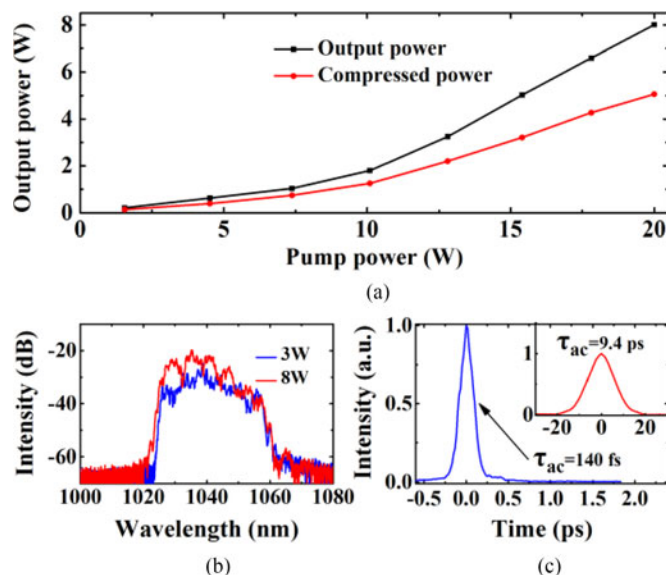
Fig. 3. (a) Output power as a function of the launched pump power. (b) Measured optical spectra of amplified signal laser with different power. (c) Autocorrelation trace of the dechirped pulse. Inset: autocorrelation trace of the direct output from the amplifier.
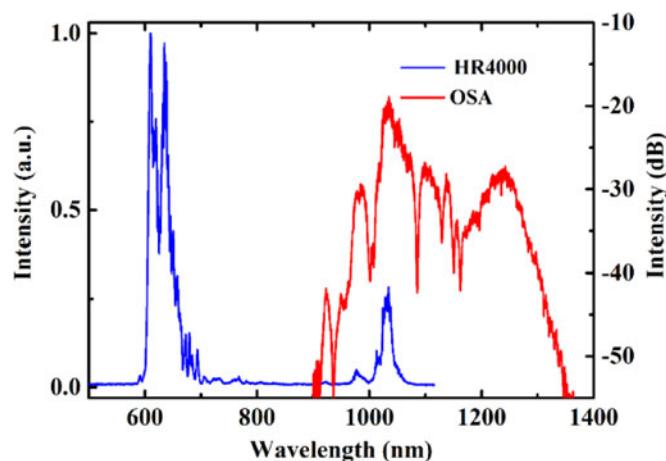

Fig. 4. SC measured by HR4000 (blue curve) from 550 to 1120 nm in linear scale and by OSA (red curve) from 800 to 1400 nm in logarithmic scale.

transform limited value (assuming Gaussian pulse). The uncompensated phase is mainly caused by the large third order dispersion (TOD) accumulated in the fibers as well as intra- and extra-cavity grating pairs.

Splitted by a beamsplitter, most of the pulse energy will be used for other applications, such as cavity-enhanced high-harmonic generation and fiber optical parameter oscillator (OPO) [34], [35]. A segment of commercial PCF (NL-3.3-890-02) with a core diameter of 3.2 μm, a zero-dispersion-wavelength at 890 nm, and a nonlinearity of 37 $W^{-1} \cdot km^{-1}$ was used for supercontinuum generation. The length of the PCF was optimized to 9 cm to maintain coherency and avoid extra nonlinearity. A 60 $\times$ objective lens was employed to couple the dechirped pulse into the PCF with 40% coupling efficiency. When the injected pulse energy reached 2 nJ, the generated SC spans from 600 to 1300 nm, as shown in Fig. 4. Two spectrometers (HR4000, Ocean optics, and AQ6370, Yokogawa) was used to record the SC.
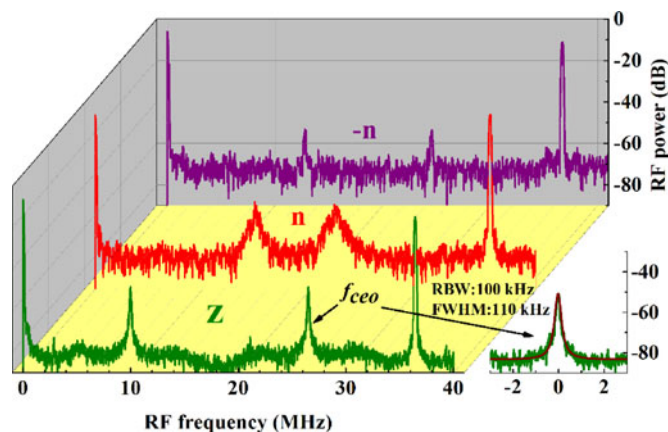
Fig. 5. SNR of the f_{ceo} signal versus net dispersion of laser oscillator. (Inset) Zoomed linewidth.

Then, a semi-collinear f-2f interferometer was used to provide the time delay between two frequency components for f_{ceo} signal. The fundamental frequency at 1240 nm being delayed was frequency-doubled by a $1 \times 9.3 \times 0.5$ mm^3 fan-out periodically-poled lithium niobate crystal and beat with the high frequency of SC at 620 nm. Fig. 5 shows the heterodyned f_{ceo} beat signal detected by a Si-avalanche photo-detector versus net dispersion of laser oscillator.

Decreasing the amplified laser power and increasing the splitting ratio, the linewidth and the SNR of the f_{ceo} signal is unchanged, indicating that this laser amplifier operated in low noise regime. The linewidth and the SNR of the free-running f_{ceo} signal varied with the net dispersion of the laser cavity. When the oscillator operated in zero dispersion regime, as much as 30-dB SNR with 110-kHz linewidth is obtained. Decreasing or increasing the net dispersion both lead to the degradation.

3. Conclusion

In conclusion, we have demonstrated that a phase-biased NALM mode-locked all-PM Yb-fiber system, delivering pulses with 140-fs pulse duration and 137-nJ pulse energy. With the assistant of an integrated phase shifter, the mode locking threshold was decreased and stable single pulse operation can be achieved by carefully decreasing pump power. Furthermore, SC spanning from 600 nm to 1300 nm was generated in a segment of nonlinear PCF and f_{ceo} signal with >30 dB SNR was detected through a semi-collinear f-2f interferometer. Hybrid multifunctional fiber components, PM fiber Bragg grating with proper negative dispersion, and a high doping concentration Yb-fiber will be considered to increase the repetition rate of the laser system. Furthermore, more work will be focused on the stabilization of both the repetition rate and the f_{ceo} signal for the expectation of a stable all PM-fiber frequency comb.

References

[1] T. Udem, R. Holzwarth, and T. W. Hansch, "Optical frequency metrology," *Nature*, vol. 416, pp. 233–237, Mar. 2002.
[2] S. A. Diddams, "The evolving optical frequency comb," *J. Opt. Soc. Amer. B*, vol. 27, pp. B51–B62, Nov. 2010.
[3] K. Minoshima and H. Matsumoto, "High-accuracy measurement of 240-m distance in an optical tunnel by use of a compact femtosecond laser," *Appl. Opt.*, vol. 39, pp. 5512–5517, Oct. 2000.
[4] K. M. T. Yamada *et al.*, "High precision line profile measurements on ^{13}C acetylene using a near infrared frequency comb spectrometer," *J. Mol. Spectrosc.*, vol. 249, pp. 95–99, Mar. 2008.
[5] G. Millot *et al.*, "Frequency-agile dual-comb spectroscopy," *Nature Photon.*, vol. 10, pp. 27–30, Dec. 2015.
[6] G. Chang, C. H. Li, D. F. Phillips, R. L. Walsworth, and F. X. Kartner, "Toward a broadband astro-comb: Effects of nonlinear spectral broadening in optical fibers," *Opt. Exp.*, vol. 18, pp. 12736–12747, Jun. 2010.
[7] L. C. Sinclair *et al.*, "Operation of an optically coherent frequency comb outside the metrology lab," *Opt. Exp.*, vol. 22, pp. 6996–7006, Mar. 2014.

[8] A. Ruehl, A. Marcinkevicius, M. E. Fermann, and I. Hartl, "80 W, 120 fs Yb-fiber frequency comb," *Opt. Lett.*, vol. 35, pp. 3015–3017, Sep. 2010.

[9] C. K. Nielsen *et al.*, "Self-starting self-similar all-polarization maintaining Yb-doped fiber laser," *Opt. Exp.*, vol. 13, pp. 9346–9351, Nov. 2005.

[10] Q. Bao *et al.*, "Atomic-layer graphene as a saturable absorber for ultrafast pulsed lasers," *Adv. Funct. Mater.*, vol. 19, pp. 3077–3083, Oct. 2009.

[11] K. Kieu and F. W. Wise, "All-fiber normal-dispersion femtosecond laser," *Opt. Exp.*, vol. 16, pp. 11453–11458, Jul. 2008.

[12] M. Chernysheva *et al.*, "Carbon nanotubes for ultrafast fibre lasers," *Nanophoton.*, vol. 6, pp. 1–30, Jan. 2017.

[13] A. Martinez and Z. Sun, "Nanotube and graphene saturable absorbers for fibre lasers," *Nature Photon.*, vol. 7, pp. 841–845, Nov. 2013.

[14] T. Kurita, H. Yoshida, T. Kawashima, and N. Miyanaga, "Generation of sub-7-cycle optical pulses from a mode-locked ytterbium-doped single-mode fiber oscillator pumped by polarization-combined 915 nm laser diodes," *Opt. Lett.*, vol. 37, pp. 3972–3974, Oct. 2012.

[15] D. Ma, Y. Cai, C. Zhou, W. Zong, L. Chen, and Z. Zhang, "37.4 fs pulse generation in an Er:fiber laser at a 225 MHz repetition rate," *Opt. Lett.*, vol. 35, pp. 2858–2860, Sep. 2010.

[16] A. Chong, W. H. Renninger, and F. W. Wise, "Environmentally stable all-normal-dispersion femtosecond fiber laser," *Opt. Lett.*, vol. 33, pp. 1071–1073, May 2008.

[17] C. K. Nielsen and S. R. Keiding, "All-fiber mode-locked fiber laser," *Opt. Lett.*, vol. 32, pp. 1474–1476, Jun. 2007.

[18] X. Shen, W. Li, and H. Zeng, "Polarized dissipative solitons in all-polarization-maintained fiber laser with long-term stable self-started mode-locking," *Appl. Phys. Lett.*, vol. 105, pp. 101109–101112, Sep. 2014.

[19] M. E. Fermann, F. Haberl, M. Hofer, and H. Hochreiter, "Nonlinear amplifying loop mirror," *Opt. Lett.*, vol. 15, pp. 752–754, Jul. 1990.

[20] P. Bowen, H. Singh, A. Runge, R. Provo, and N. G. R. Broderick, "Mode-locked femtosecond all-normal all-PM Yb-doped fiber laser at 1060 nm," *Opt. Commun.*, vol. 364, pp. 181–184, Dec. 2016.

[21] F. O. Ilday, F. W. Wise, and T. Sosnowski, "High-energy femtosecond stretched-pulse fiber laser with a nonlinear optical loop mirror," *Opt. Lett*, vol. 27, pp. 1531–1533, Sep. 2002.

[22] J. Szczepanek, T. M. Kardaś, M. Michalska, C. Radzewicz, and Y. Stepanenko, "Simple all-PM-fiber laser mode-locked with a nonlinear loop mirror," *Opt. Lett.*, vol. 40, pp. 3500–3503, Aug. 2015.

[23] M. Erkintalo, C. Aguergaray, A. Runge, and N. G. R. Broderick, "Environmentally stable all-PM all-fiber giant chirp oscillator," *Opt. Exp.*, vol. 20, pp. 22669–22674, Sep. 2012.

[24] Q. Hao, F. Chen, K. Yang, X. Zhu, Q. Zhang, and H. Zeng, "Self-started mode-locking with dispersion-imbalanced nonlinear amplifier loop," *IEEE Photon. Technol. Lett.*, vol. 28, no. 1, pp. 87–90, Jan. 2016.

[25] M. E. Fermann, L. Turi, M. Hofer, F. Haberl, and A. J. Schmidt, "Additive-pulse-compression port of a neodymium fiber laser," *Opt. Lett.*, vol. 16, pp. 244–246, Feb. 1991.

[26] J. W. Nicholson and M. Andrejco, "A polarization maintaining, dispersion managed, femtosecond figure-eight fiber laser," *Opt. Exp.*, vol. 14, pp. 8160–8167, Sep. 2006.

[27] Q. Hao, Q. Zhang, F. Chen, K. Yang, and H. Zeng, "All-optical 20-μHz-level repetition rate stabilization of mode locking with a nonlinear amplifying loop mirror," *J. Lightw. Technol.*, vol. 34, no. 11, pp. 2833–2837, Jun. 2016.

[28] H. Lin, D. K. Donald, and W. V. Sorin, "Optimizing polarization states in a figure-8 laser using a nonreciprocal phase shifter," *J. Lightw. Technol.*, vol. 12, no. 7, pp. 1121–1128, Jul. 1994.

[29] W. Hänsel, R. Holzwarth, R. Doubek, and M. Mei, "Laser with non-linear optical loop mirror," EP Patent EP 2 637 265 A1, Sep. 11, 2013. [Online]. Available: https://www.google.com/patents/ EP2637265A1?cl=en

[30] N. Kuse, J. Jiang, C. C. Lee, T. R. Schibli, and M. E. Fermann, "All polarization-maintaining Er fiber-based optical frequency combs with nonlinear amplifying loop mirror," *Opt. Exp.*, vol. 24, pp. 3095–3102, Feb. 2016.

[31] T. Jiang, Y. Cui, P. Lu, C. Li, A. Wang, and Z. Zhang, "All PM fiber laser mode locked with a compact phase biased amplifier loop mirror," *IEEE Photon. Technol. Lett.*, vol. 28, no. 16, pp. 1786–1789, Aug. 2016.

[32] L. Zhang, J. Zhou, Z. Wang, X. Gu, and Y. Feng, "SESAM mode-locked, environmentally stable, and compact dissipative soliton fiber laser," *IEEE Photon. Technol. Lett.*, vol. 26, no. 13, pp. 1314–1316, Jul. 2014.

[33] L. Nugent-Glandorf, T. A. Johnson, Y. Kobayashi, and S. A. Diddams, "Impact of dispersion on amplitude and frequency noise in a Yb-fiber laser comb," *Opt. Lett.*, vol. 36, pp. 1578–1580, May 2011.

[34] T. Südmeyer *et al.*, "Femtosecond fiber-feedback optical parametric oscillator," *Opt. Lett.*, vol. 26, pp. 304–306, Mar. 2001.

[35] T. Gottschall *et al.*, "Fiber-based optical parametric oscillator for high resolution coherent anti-Stokes Raman scattering (CARS) microscopy," *Opt. Exp.*, vol. 22, pp. 21921–21928, Sep. 2014.